UDC 621.3 https://doi.org/10.20998/2074-272X.2024.1.02

G. Srinivas, G. Durga Sukumar, M. Subbarao

# Total harmonic distortion analysis of inverter fed induction motor drive using neuro fuzzy type-1 and neuro fuzzy type-2 controllers

***Introduction.*** *When the working point of the indirect vector control is constant, the conventional speed and current controllers operate effectively. The operating point, however, is always shifting. In a closed-system situation, the inverter measured reference voltages show higher harmonics. As a result, the provided pulse is uneven and contains more harmonics, which enables the inverter to create an output voltage that is higher.* ***Aim.*** *A space vector modulation (SVM) technique is presented in this paper for type-2 neuro fuzzy systems. The inverter's performance is compared to that of a neuro fuzzy type-1 system, a neuro fuzzy type-2 system, and classical SVM using MATLAB simulation and experimental validation.* ***Methodology.*** *It trains the input-output data pattern using a hybrid-learning algorithm that combines back-propagation and least squares techniques. Input and output data for the proposed technique include information on the rotation angle and change of rotation angle as input and output of produced duty ratios. A neuro fuzzy-controlled induction motor drive's dynamic and steady-state performance is compared to that of the conventional SVM when using neuro fuzzy type-2 SVM the induction motor, performance metrics for current, torque, and speed are compared to those of neuro fuzzy type-1 and conventional SVM.* ***Practical value.*** *The performance of an induction motor created by simulation results are examined using the experimental validation of a dSPACE DS-1104. For various switching frequencies, the total harmonic distortion of line-line voltage using neuro fuzzy type-2, neuro fuzzy type-1, and conventional based SVMs are provided. The 3 hp induction motor in the lab is taken into consideration in the experimental validations.* References 22, tables 3, figures 15.
*Key words*: **space vector modulation, neuro fuzzy type-1, neuro fuzzy type-2, induction motor, total harmonic distortion.**

***Вступ***. *Коли робоча точка непрямого векторного управління стала, традиційні регулятори швидкості та струму працюють ефективно. Проте робоча точка постійно змінюється. У ситуації закритої системи виміряна інвертором опорна напруга показує вищі гармоніки. В результаті імпульс, що подається, нерівномірний і містить більше гармонік, що дозволяє інвертору створювати більш високу вихідну напругу.* ***Мета***. *У цій статті представлена методика просторової векторної модуляції (SVM) для нейронечітких систем типу 2. Продуктивність інвертора порівнюється з продуктивністю нейронечіткої системи типу 1, нейронечіткої системи типу 2 та класичної SVM з використанням моделювання MATLAB та експериментальної перевірки.* ***Методологія***. *Навчається шаблон даних введення-виводу, використовуючи алгоритм гібридного навчання, який поєднує у собі методи зворотного поширення помилки та методу найменших квадратів. Вхідні та вихідні дані для запропонованої методики включають інформацію про кут повороту і зміну кута повороту як отримані вхідні і вихідні коефіцієнти заповнення. Динамічні характеристики приводу асинхронного двигуна з нейронечітким управлінням порівнюються з характеристиками звичайного SVM. При використанні нейронечіткого SVM типу 2 асинхронний двигун, показники продуктивності по струму обертаючого моменту і швидкості порівнюються з показниками приводу асинхронного двигуна з нейронечітким управлінням типу 1 та традиційного SVM.* ***Практична цінність***. *Продуктивність асинхронного двигуна, створеного за результатами моделювання, досліджується з використанням експериментальної перевірки dSPACE DS-1104. Для різних частот перемикання розраховуються загальні гармонічні спотворення лінійної напруги з використанням нейронечіткого управління типу 2, нейронечіткого управління типу 1 і традиційного SVM. Асинхронний двигун потужністю 3 л.с. у лабораторії враховується під час експериментальних перевірок.* Бібл. 22, табл. 3, рис. 15.
*Ключові слова:* **просторово-векторна модуляція, нейронечіткий тип 1, нейронечіткий тип 2, асинхронний двигун, повне гармонійне спотворення.**

**1. Introduction.** Space vector modulation (SVM) is a technique for managing the pulse width modulation method used to regulate the inverter-fed induction motor (IM). At the turning points, which are caused by space vector instants, the pulse width modulated voltage source inverter is used. In compared to the straightforward sinusoidal approach, switching times are reduced and current and torque ripple are decreased [1]. For both linear and non-linear modes of operation, the digital implementation is a technique utilized in transient simulation. SVM is a method for implementing optimum bus voltage utilization and support for the harmonic spectrum utilized in current applications is explained in [2]. To reduce ripple in torque and current, the adaptive neuro fuzzy interference system based on maximum power point tracking is presented for IM driving in MATLAB/Simulink and is confirmed using an experimental setup utilising the hardware D-space (1104) is discuss in [3]. The type-2 fuzzy logic direct torque control technique is implemented because of the replacement of proportional-integral controllers. Using the control technique, the reaction improved in both transient and steady state conditions. Under various operating conditions, it also reduces torque ripple and flux distortion in contrast to the regular direct torque control [4]. Instead of using filters to reduce torque ripple like standard propositional integral controllers, adaptive neuro fuzzy interference system current controllers are employed for an indirect vector of an inverter driven IM. The performance of the drive is simulated under various operating conditions [5].To reduce switching losses and output voltage distortion from the created SVM algorithm, the proposed method uses variable frequency modulation to voltage source inverter fed IM [6]. Instead of a proposal integral controller with no filter, a neuro fuzzy torque controller is employed to eliminate torque ripple. The SVM approach is also suggested, although information is required to calculate the sector and angle [7]. For the error inside the boundary, an *n*-level voltage source inverter fed with current error space vector hysteresis is used as the current controller. The advantage of the hysteresis controller is that it transitions from linear to over modulation smoothly. It has also been confirmed by experimental validation with steady and transient performances. [8]. For the voltage source inverter fed IM drive, type-2 fuzzy-based methodology has been used. The technique has been compared to traditional SVM for performance and is independent of switching frequency. [9]. The adaptive-

network-based fuzzy inference system based SVM is not required to predict the switching frequency or required training error when using the SVM method. This is the reason why, in contrast to other optimization strategies like genetic, neural and fuzzy [10]. The development of a technology known as constant switching frequency torque control can be used to manage torque in both steady state and dynamic conditions. For calculating the torque ripple and angular velocity, it employs flux error vector-based SVM [11]. Fast switching frequency is implemented using the artificial neural network SVM based fed voltage source inverter, which leads to dynamic operation of the IM drive under linear region to square wave. [12]. SVM based on neuro fuzzy and three-level inverter fed voltage source used to implement improved constant and dynamic performance of the IM drive. The suggested method generates an output with the proper duty ratios by changing the input space-vector angle. The neural network with a specific integrated circuit chip is used to easily implement the SVM algorithm. [13, 14].The recommended artificial neural network with SVM-based voltage source inverter fed IM drive estimate a variety of outputs without regard to switching frequency [15]. The five-layer network fed into the neuro fuzzy SVM-based inverter produces output that is trained duty ratios from input from $V_{ds}$ and $V_{qs}$. Simulation and experimental validation can be used to estimate the total harmonic distortion (THD) computation for various switching frequencies [16]. For a wind turbine with a doubly fed induction generator, use SVM. The method is used for minimizing the harmonic distortion of stator currents under various wind speed [17].

**2. Mathematical modelling of IM.** Using direct-quadrature (*d-q*) stationary references, a mathematical model of a three-phase squirrel cage IM was developed [18].

$$\frac{\mathrm{d}i_{ds}}{\mathrm{d}t} = -\frac{1}{\sigma L_s}\left(R_s + \frac{L_m^2}{L_r^2}\right) i_{ds} + \frac{1}{\sigma L_s}\frac{L_m R_r}{L_r^2}\psi_{dr} + \\ + \frac{pL_m}{\sigma L_s L_r}\omega_r \psi_{dr} + \frac{V_{ds}}{\sigma L_s}; \quad (1)$$

$$\frac{\mathrm{d}i_{qs}}{\mathrm{d}t} = -\frac{1}{\sigma L_s}\left(R_s + \frac{L_m^2}{L_r^2}R_r\right) i_{qs} + \frac{1}{\sigma L_s}\frac{L_m R_r}{L_r^2}\psi_{qr} - \\ - \frac{pL_m}{\sigma L_s L_r}\omega_r \psi_{dr} + \frac{V_{qs}}{\sigma L_s}; \quad (2)$$

$$\frac{\mathrm{d}\psi_{dr}}{\mathrm{d}t} = -\frac{R_r}{L_r}\psi_{dr} - p\omega_r \psi_{qr} + \frac{L_m R_r}{L_r} i_{ds}; \quad (3)$$

$$\frac{\mathrm{d}\psi_{qr}}{\mathrm{d}t} = -\frac{R_r}{L_r}\psi_{qr} + p\omega_r \psi_{dr} + \frac{L_m R_r}{L_r} i_{qs}; \quad (4)$$

$$\frac{\mathrm{d}\omega_r}{\mathrm{d}t} = -\frac{B}{J}\omega_r + \frac{1}{J}(T_e - T_l), \quad (5)$$

where $\sigma = (1 - L_m^2 / L_s L_r)$ is the leakage coefficient; $i_{ds}$, $i_{dr}$ are the stator currents of *d-q* axis; $R_s$, $R_r$ are the stator and rotor resistances; $V_{ds}$, $V_{dr}$ are the stator voltage of *d-q* axis; $L_s$, $L_r$ are the stator and rotor inductances; $\psi_{ds}$, $\psi_{dr}$ are the rotor fluxes of *d-q* axis; $L_m$, $\omega_r$, $p$ are the magnetizing inductance, rotor speed and number of poles; $B$ is the damping coefficient; $J$ is the moment of inertia; $T_e$, $T_l$ are the electromagnetic and load torques.

**3. Mathematically modulated two level inverter.** Variable speed drives use pulse width modulation, which is regulated using a method known as space vector. The states of a two-level inverter are flipped using these various vectors. The connection diagram of two level inverter and space vector diagram is presented in Fig. 1. Choosing the $V_0$ and $V_7$ vectors results in a voltage that is zero. The remaining vectors $V_1$ to $V_6$ are chosen to provide the induction machine with the necessary voltage.

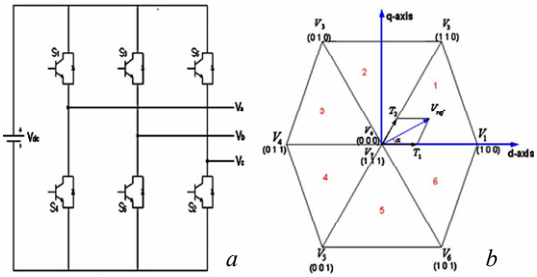


Fig. 1 Two level inverter (*a*) and space vector diagram with active vectors (*b*)

The reference voltage $V_{ref}$, which has a constant value, is created by combining the nearest two active vectors $V_n$ and $V_{n+1}$, with zero vectors ($V_0$ and $V_7$). By merging two active vectors, effective vectors can be employed to achieve the desired results. The block diagram of proposed SVM based inverter control using neuro fuzzy type-2 (NFT2) is shown in Fig. 2.

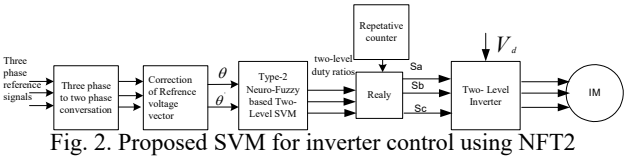


Fig. 2. Proposed SVM for inverter control using NFT2

The following can be inferred from mentioned concept of the necessary mean voltage and unit sample time for the reference vector:

$$V_{ref} = (T_1 V_n + T_2 V_{n+1}) / T_s, \quad (7)$$

where $T_1$, $T_2$ represent the $V_1$-$V_6$ sector's active times.

While the equation are being equated, along the direct axis is

$$V_{ref} \cos\alpha T_s = V_{dc} T_1 + (V_{dc} \cos(\pi/3)) T_2. \quad (8)$$

As the equation are being equated along the quadrature axis:

$$V_{ref} \sin\alpha T_s = V_{dc} T_1 + (V_{dc} \sin(\pi/3)) T_2, \quad (9)$$

where $V_{dc}$ is the magnitude of each active vector; $V_{ref}$ is the angle of 60° sector with respect to the sector's beginning $V_1$-$V_6$;

$$T_1 = M \frac{\sin(\pi/3 - \alpha)}{\sin(\pi/3)} T_s; \quad (10)$$

$$T_2 = M \frac{\sin\alpha}{\sin(\pi/3)} T_s; \quad (11)$$

$$T_0 = T_s - T_1 - T_2, \quad (12)$$

where $T_s$ is the sampling period; $T_0$ is the duration of zero vector and $M$ is the modulation index and is given by $V_{ref}/V_{dc}$. The ripple value decreases to zero when time is divided uniformly.

**4. Modified NFT2 based SVM.** In order to develop a NFT2 system, the IF-THEN rules are used which have antecedent and consequent sections with type-2 fuzzy values. Uncertainties in fuzzy sets of Gaussian type-2 can be connected to the mean and standard deviation.

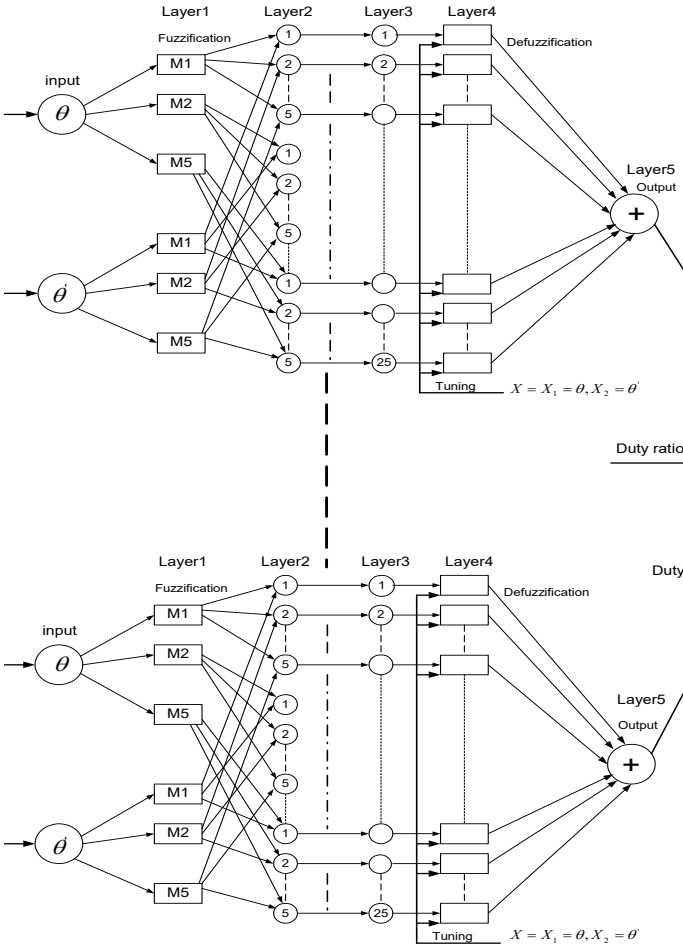


A fuzzy inference system's hardware implementation comprises of implementing the fuzzification, fuzzy inferences, and defuzzification discussed in [19]. The duty ratios are generated using a NFT2 based SVM that has been trained in the under modulation zone. The switching frequencies are 3 kHz and 15 kHz. The training data for NFT2 interference system obtained simulating the conventional SVM [20]. Typically, training takes from 0 to 5 min each epoch on a 1.8 GHz Pentium Dual Core computer, with a training error of less than 0.0002.

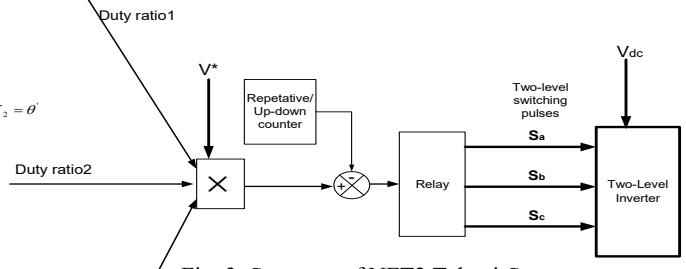


Fig. 3. Structure of NFT2 Takagi-Sugeno system

The input variables $\theta$ (space vector) and $\theta'$ (change of space vector) each have a number membership function of 5 and 5, respectively (see Fig. 3). So, there are we have 25 rules (5·5 = 25). For two input variables, Bell shape membership functions are employed. As a result, NFT2 are 105 fitting parameters overall. Because the premise parameters are 30 (5·3+5·3 = 30) and the consequent parameters are 75 (3·25 = 75).

**5. Results and discussions.** In the direct torque control concept, using a proportional integral speed controller causes a loss of decoupling with respect to parameter fluctuations [21]. The performance characteristics of an IM have been studied using proportional integral, neuro fuzzy type-1 (NFT1), and NFT2 SVM-based controllers in a different operating condition, i.e. steady state and step change. The command speed of the 3 hp IM is 157 rad/s (1500 rpm). The parameters of the IM are shown in Table 1.

Table 1

Parameters of the IM

| | |
|---|---|
| Motor power | 2.2 kW (3 hp), 400 V |
| Number of the poles $p$ | 4 |
| Inverter switching frequencies, kHz | 3 and 15 |
| DC link voltage, V | 150 |
| Modulation index | 0.86 |
| Stator resistance $R_s$, Ω | 0.55 |
| Stator inductance $L_s$, mH | 93.38 |
| Rotor resistance $R_r$, Ω | 0.78 |
| Rotor inductance $L_r$, mH | 93.36 |
| Magnetizing inductance $L_m$, mH | 90.5 |
| Moment of inertia $J$, kg·m$^2$ | 0.019 |
| Damping coefficient $B$ | 5·10$^{-5}$ |

**5.1 Inverter line-to-line voltage and harmonic spectrum switching frequency of 3 kHz.**

For DC link voltage 150 V the fundamental line voltage increased by 0.56 % in NFT2 as compared with conventional based SVM (see Fig. 4,*a*,*c*) and 0.44 % increased as compared NFT1 based SVM (see Fig. 4,*b*,*c*).

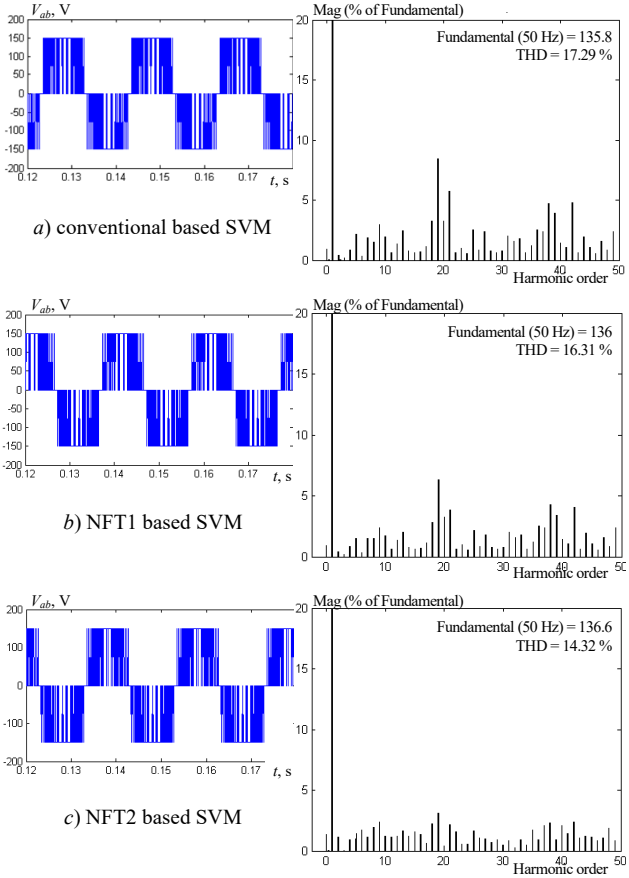


*a*) conventional based SVM

*b*) NFT1 based SVM

*c*) NFT2 based SVM

Fig. 4. Inverter line to-line voltage and harmonic spectrum at switching frequency of 3 kHz

In comparison to NFT1 SVM and conventional SVM, the 5th and 7th harmonics are decreased in NFT2 SVM. Comparing NFT2 based SVM to NFT1 based SVM and conventional SVM, the THD was also lowered (see Table 2)

Table 2

THD comparison at 3 kHz

| No | Parameter | Conventional SVM | NFT1 based SVM | NFT2 based SVM |
|---|---|---|---|---|
| 1 | Fundamental line voltage (peak), V | 135.8 | 136 | 136.6 |
| 2 | 5th harmonic, % | 2.13 | 1.98 | 1.87 |
| 3 | 7th harmonic, % | 1.86 | 1.55 | 1.1 |
| 4 | THD, % | 17.29 | 16.31 | 14.32 |

**5.2 Performance of IM (switching frequency 3 kHz).**

**1. Operation during steady state.** IM steady state torque ripple decreased from 2.2 N·m to 1 N·m in NFT2 based SVM as compared to conventional based SVM (see Fig. 5,*a*,*c*). Similarly, torque ripple reduced from 2.2 N·m to 2 N·m in NFT2 as compared with NFT1 based SVM (see Fig. 5,*b*,*c*). The speed response reaches early in NFT2 based SVM compared with NFT1 and conventional based SVM (see Fig. 5,*c*). SVM technique and fuzzy logic control are used in two distinct direct torque control methods, which are described in [22].

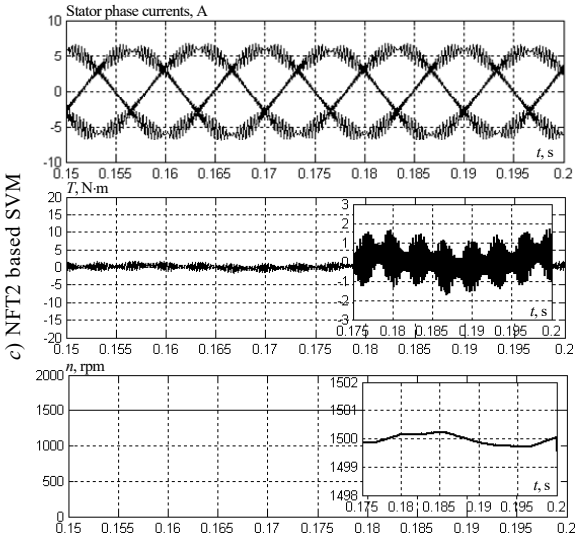


Fig. 5. IM performance at 3 kHz during steady state operation

**2. During step change operation.** When compared to conventional SVM, an IM is operating during a step change, the torque ripple is reduced from 17.5 N·m to 15 N·m in NFT2 based SVM (see Fig. 6,*a*,*c*). Similarly as compared to NFT1 based SVM, torque ripple reduced from 17 N·m to 15 N·m (see Fig. 6,*b*,*c*).

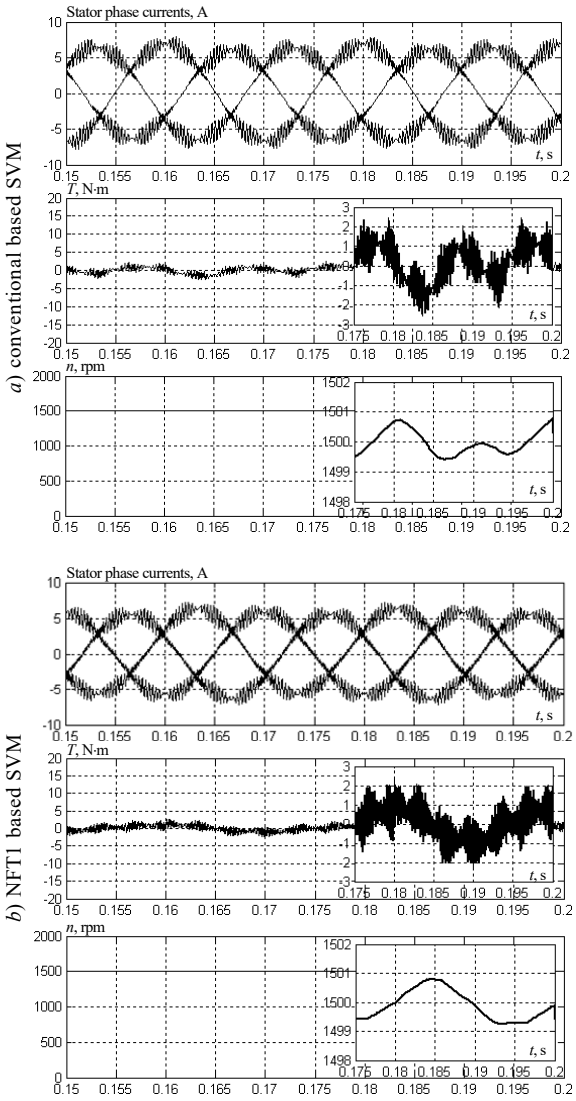


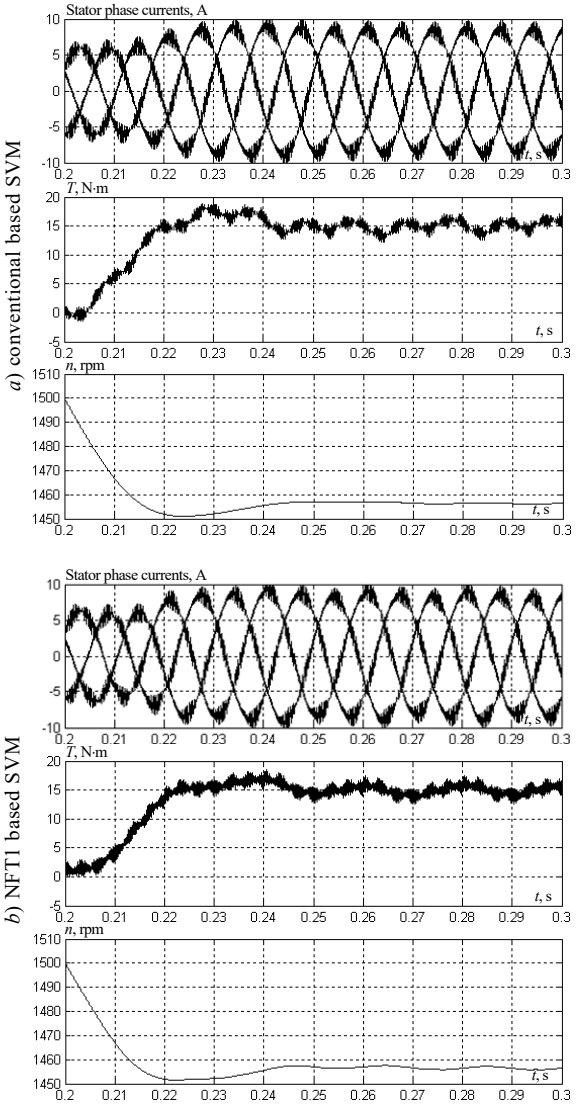

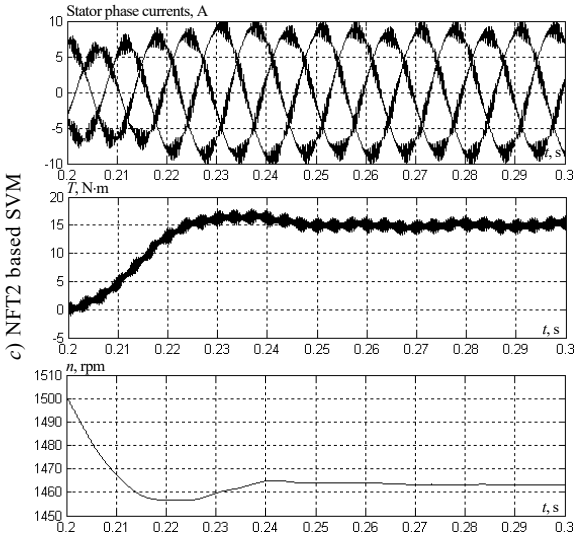


Fig. 6. Performance of a step change IM running at 3 kHz

The torque ripple reduced by 16.66 % in NFT2 based SVM. When compared to NFT1 and conventional SVM, the stator current increased by 33.33 % in NFT2 based SVM (Fig. 6,*c*). The quick response arrives before time (see Fig. 6,*c*).

**5.3 Inverter line-to-line voltage and harmonic spectrum at switching frequency of 15 kHz.**

The fundamental line voltage increased by 0.87 % in NFT2 as compared with conventional SVM (see Fig. 7,*a*,*c*).

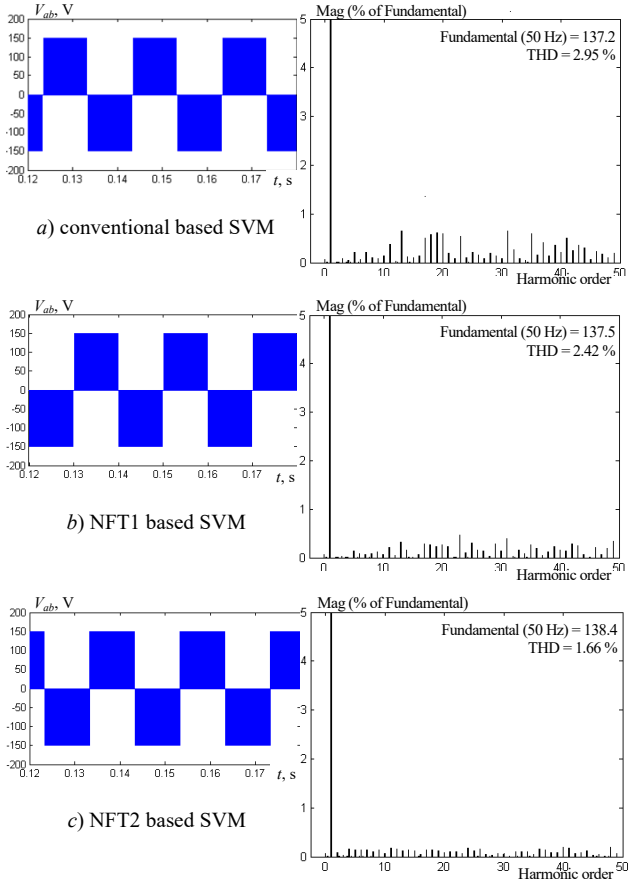


Fig. 7. Inverter line-to-line voltage and harmonic spectrum at switching frequency of 15 kHz

Similarly, in NFT2 based SVM the fundamental line voltage increased by 0.65 % as compared with NFT1 based SVM (see Fig. 7,*b*,*c*). For a 150 V DC inverter, NFT2 based SVM reduces the 5th and 7th harmonic as comparing with conventional and NFT1 based SVM, the overall THD was similarly lower (see Table 3).

Table 3

Comparison of THD at 15 kHz

| No | Parameter | Conventional SVM | NFT1 based SVM | NFT2 based SVM |
|---|---|---|---|---|
| 1 | Fundamental line voltage (peak), V | 137.2 | 137.5 | 138.4 |
| 2 | 5th harmonic, % | 1.2 | 0.2 | 0.14 |
| 3 | 7th harmonic, % | 0.47 | 0.31 | 0.06 |
| 4 | THD, % | 2.95 | 2.42 | 1.66 |

**5.4 Performance of IM (switching frequency 15 kHz). Operation during steady state.** When compared to conventional SVM, the torque ripple caused by an IM operating in steady state is reduced (1.5 N·m to 0.5 N·m) by 66.665 % in NFT2 (see Fig. 8,*a*,*c*). Similarly, in NFT2 based SVM, the ripple in torque reduced (0.8 N·m to 0.5 N·m) by 0.375 % as compared with NFT1 based SVM (see Fig. 8,*b*,*c*). The ripple in the stator current was also reduced by 0.37 %, and the speed response arrived earlier (see Fig. 8,*c*).

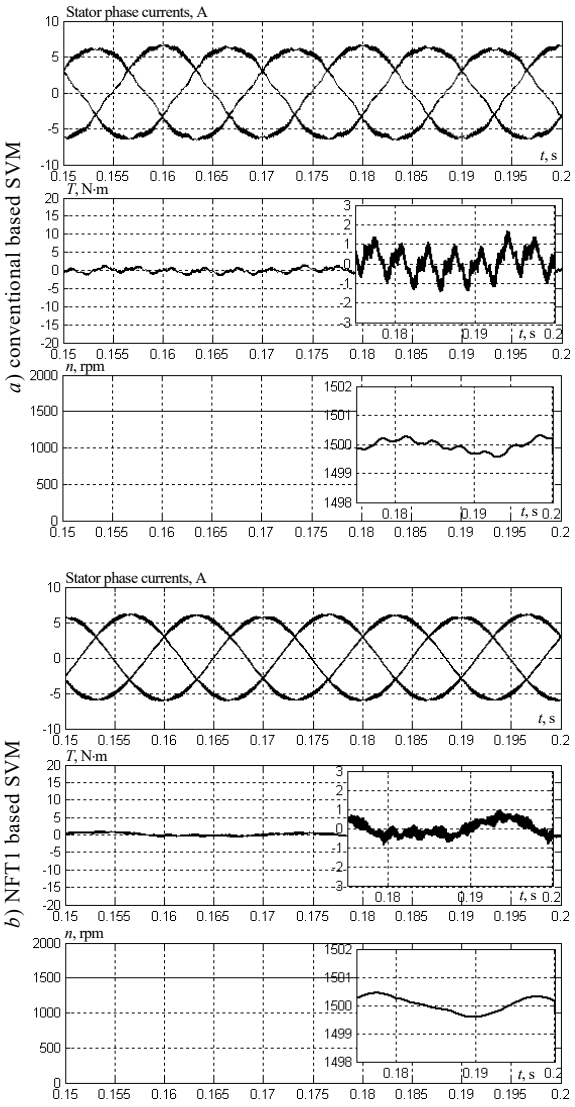

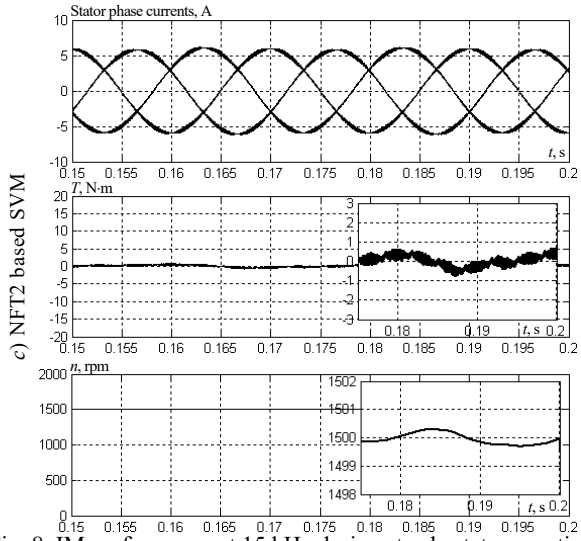

Fig. 8. IM performance at 15 kHz during steady state operation

**6. Experimental validation.** A dSPACE DS-1104 is employed to carry out the NFT2 based SVM algorithm in real time. The initial development of the control algorithm takes place in MATLAB/Simulink. By using MATLAB's real time workshop, automatic *C* code generation for real time implementation is accomplished. The experimental setup is shown in Fig. 9.

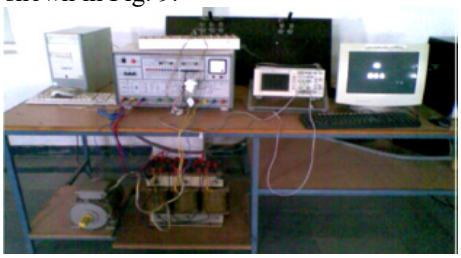
Fig. 9. Experimental setup

**6.1 Line–to-line voltage at 3 kHz.** The THD value also reduced in NFT2 based SVM as compared with NFT1 based SVM and conventional SVM (Fig. 10-12, where 1 div is 50 V).

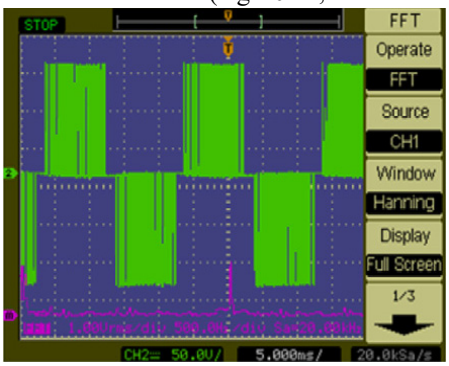

Fig. 10. Conventional SVM

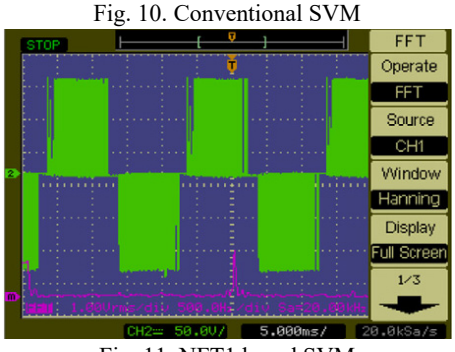

Fig. 11. NFT1 based SVM

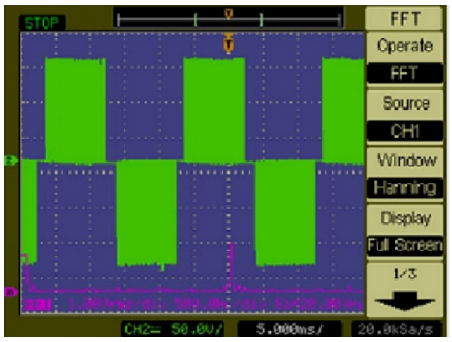

Fig. 12. NFT2 based SVM

**6.2 Speed response of IM drive.** Finally, Fig. 13-15 present the speed response reaches early in NFT2 based SVM as compared with NFT1 based SVM and conventional based SVM. The performance of IM drive improved under steady state operation and step change operation.

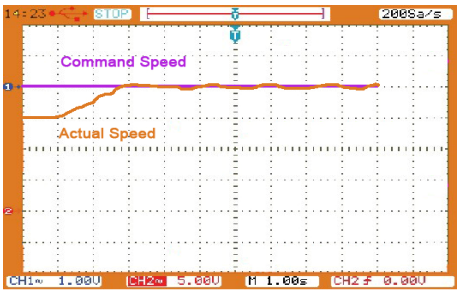

Fig. 13. Conventional based SVM

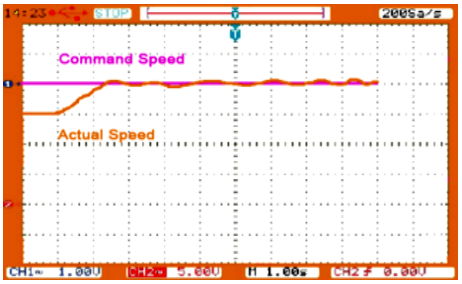

Fig. 14. NFT1 based SVM

Fig. 15. NFT2 based SVM

**7. Conclusions.** A dynamic response of the induction motor (IM) has been seen while comparing the recommended neuro fuzzy type-2 (NFT2) space vector modulation (SVM) based controller to the conventional based SVM and neuro fuzzy type-1 (NFT1) based SVM controllers.

The performance of NFT1 controllers based SVM IM drive under various operating conditions with switching frequency at 3 and 15 kHz examined. The fundamental line voltage is 0.14 % increase in NFT1 based SVM as compared with conventional SVM. The $5^{th}$, $7^{th}$ harmonic components are reduced by 7.04 %, 16.66 % respectively in NFT1 based SVM as compared with conventional SVM. The total harmonic distortion (THD) in NFT1 based SVM reduced by 5.66 % as compared with conventional SVM.

Similarly, IM drive operates under 15 kHz operation the fundamental line voltage is increased by 0.21 % as compared with conventional SVM. The $5^{th}$ , $7^{th}$ harmonic components are reduced by 83.33 %, 34.04 % respectively in NFT1 based SVM as compared with conventional SVM. The THD in NFT1 based SVM reduced by 17.96 % as compared with conventional SVM.

The experimental implementation of the IM drive with conventional SVM, NFT1 and NFT2 controllers based SVM examine at switching frequency 3 kHz using dSPACE DS-1104. The inverter line voltage $V_{ab}$ THD value reduced by 23.1 %, 9.65 % in NFT2 SVM by as compared with conventional SVM, NFT1 SVM respectively. The inverter line voltage $V_{bc}$ THD value is reduced by 18.9 % in NFT2 SVM by as compared with conventional SVM. The inverter line voltage $V_{ca}$ THD value is reduced by 23.1 %, 9.65 % in NFT2 SVM by as compared with conventional SVM, NFT1 SVM respectively.

The dynamic performance of IM drive improved with NFT2 based SVM as compared with NFT1 and conventional based SVM.

**Conflict of interest**: The authors declare that they have no conflicts of interest.

REFERENCES


***1.*** Van der Broeck H.W., Skudelny H.-C., Stanke G.V. Analysis and realization of a pulsewidth modulator based on voltage space vectors. *IEEE Transactions on Industry Applications*, 1988, vol. 24, no. 1, pp. 142-150. doi: https://doi.org/10.1109/28.87265.

***2.*** Mehrizi-Sani A., Filizadeh S. Digital implementation and transient simulation of space-vector modulated converters. *2006 IEEE Power Engineering Society General Meeting*, 2006, pp. 1-7. doi: https://doi.org/10.1109/PES.2006.1709108.

***3.*** Pakkiraiah B., Durga Sukumar G. Enhanced Performance of an Asynchronous Motor Drive with a New Modified Adaptive Neuro-Fuzzy Inference System-Based MPPT Controller in Interfacing with dSPACE DS-1104. *International Journal of Fuzzy Systems*, 2017, vol. 19, no. 6, pp. 1950-1965. doi: https://doi.org/10.1007/s40815-016-0287-5.

***4.*** Venkataramana Naik N., Singh S.P. Improved Torque and Flux Performance of Type-2 Fuzzy-based Direct Torque Control Induction Motor Using Space Vector Pulse-width Modulation. *Electric Power Components and Systems*, 2014, vol. 42, no. 6, pp. 658-669. doi: https://doi.org/10.1080/15325008.2013.871608.

***5.*** Durgasukumar G., Pathak M.K. Neuro-fuzzy-based torque ripple reduction and performance improvement of VSI fed induction motor drive. *International Journal of Bio-Inspired Computation*, 2012, vol. 4, no. 2, pp. 63-72. doi: https://doi.org/10.1504/IJBIC.2012.047174.

***6.*** Attaianese C., Nardi V., Tomasso G. Space Vector Modulation Algorithm for Power Losses and THD Reduction in VSI Based Drives. *Electric Power Components and Systems*, 2007, vol. 35, no. 11, pp. 1271-1283. doi: https://doi.org/10.1080/15325000701351724.

***7.*** Durgasukumar G., Pathak M.K. Neuro-fuzzy-based space vector modulation for THD reduction in VSI fed induction motor drive. *International Journal of Power Electronics*, 2012, vol. 4, no. 2, pp. 160-180. doi: https://doi.org/10.1504/IJPELEC.2012.045629.

***8.*** Dey A., Rajeevan P.P., Ramchand R., Mathew K., Gopakumar K. A Space-Vector-Based Hysteresis Current Controller for a General n-Level Inverter-Fed Drive With Nearly Constant Switching Frequency Control. *IEEE Transactions on Industrial Electronics*, 2013, vol. 60, no. 5, pp. 1989-1998. doi: https://doi.org/10.1109/TIE.2012.2200217.

***9.*** Durgasukumar G., Abhiram T., Pathak M.K. TYPE-2 Fuzzy based SVM for two-level inverter fed induction motor drive. *2012 IEEE 5th India International Conference on Power Electronics (IICPE)*, 2012, pp. 1-6. doi: https://doi.org/10.1109/IICPE.2012.6450468.

***10.*** Durgasukumar G., Ramanjan Prasad R. Torque ripple minimization of vector controlled VSI Induction Motor Drive using Neuro-Fuzzy Controller. *International Journal of Advances in Engineering Sciences*, 2011, vol. 1, no. 1, pp. 40-43.

***11.*** Tripathi A., Khambadkone A.M., Panda S.K. Torque Ripple Analysis and Dynamic Performance of a Space Vector Modulation Based Control Method for AC-Drives. *IEEE Transactions on Power Electronics*, 2005, vol. 20, no. 2, pp. 485-492. doi: https://doi.org/10.1109/TPEL.2004.842956.

***12.*** Kazmierkowski M.P., Da Silva L.E.B., Bose B.K., Pinto J.O.P. A neural-network-based space-vector PWM controller for voltage-fed inverter induction motor drive. *IEEE Transactions on Industry Applications*, 2000, vol. 36, no. 6, pp. 1628-1636. doi: https://doi.org/10.1109/28.887215.

***13.*** Sukumar D., Jithendranath J., Saranu S. Three-level Inverter-fed Induction Motor Drive Performance Improvement with Neuro-fuzzy Space Vector Modulation. *Electric Power Components and Systems*, 2014, vol. 42, no. 15, pp. 1633-1646. doi: https://doi.org/10.1080/15325008.2014.927022.

***14.*** Mondal S.K., Pinto J.O.P., Bose B.K. A neural-network-based space-vector PWM controller for a three-level voltage-fed inverter induction motor drive. *IEEE Transactions on Industry Applications*, 2002, vol. 38, no. 3, pp. 660-669. doi: https://doi.org/10.1109/TIA.2002.1003415.

***15.*** Muthuramalingam A., Sivaranjani D., Himavathi S. Space Vector Modulation of a Voltage fed Inverter Using Artificial Neural Networks. *2005 Annual IEEE India Conference - Indicon*, 2005, pp. 487-491. doi: https://doi.org/10.1109/INDCON.2005.1590218.

***16.*** Durgasukumar G., Pathak M.K. Comparison of adaptive Neuro-Fuzzy-based space-vector modulation for two-level inverter. *International Journal of Electrical Power & Energy Systems*, 2012, vol. 38, no. 1, pp. 9-19. doi: https://doi.org/10.1016/j.ijepes.2011.10.017.

***17.*** Boukadoum A., Bouguerne A., Bahi T. Direct power control using space vector modulation strategy control for wind energy conversion system using three-phase matrix converter. *Electrical Engineering & Electromechanics*, 2023, no. 3, pp. 40-46. doi: https://doi.org/10.20998/2074-272X.2023.3.06.

***18.*** Diab A.A.Z., Elsawy M.A., Denis K.A., Alkhalaf S., Ali Z.M. Artificial Neural Based Speed and Flux Estimators for Induction Machine Drives with Matlab/Simulink. *Mathematics*, 2022, vol. 10, no. 8, art. no. 1348. doi: https://doi.org/10.3390/math10081348.

***19.*** Aib A., Khodja D.E., Chakroune S. Field programmable gate array hardware in the loop validation of fuzzy direct torque control for induction machine drive. *Electrical Engineering & Electromechanics*, 2023, no. 3, pp. 28-35. doi: https://doi.org/10.20998/2074-272X.2023.3.04.

***20.*** Srinivas G., Sukumar G.D. A modified type-2 neuro-fuzzy SVM-based inverter fed IM drive. International *Journal of Power Electronics*, 2022, vol. 15, no. 3/4, pp. 267-289. doi: https://doi.org/10.1504/IJPELEC.2022.122406.

***21.*** Guezi A., Bendaikha A., Dendouga A. Direct torque control based on second order sliding mode controller for three-level inverter-fed permanent magnet synchronous motor: comparative study. *Electrical Engineering & Electromechanics*, 2022, no. 5, pp. 10-13. doi: https://doi.org/10.20998/2074-272X.2022.5.02.

***22.*** Moussaoui L. Performance enhancement of direct torque control induction motor drive using space vector modulation strategy. *Electrical Engineering & Electromechanics*, 2022, no. 1, pp. 29-37. doi: https://doi.org/10.20998/2074-272X.2022.1.04.



*Received 03.06.2023*
*Accepted 30.08.2023*
*Published 02.01.2024*



*G. Srinivas*[1], *Research Scholar*,
*G. Durga Sukumar*[2], *Professor*,
*M. Subbarao*[1], *Associative Professor*,
[1] Electrical and Electronics Engineering Department,
Vignan's Foundation for Science, Technology and Research University, Vadlamudi, Guntur 522213, India,
e-mail: gadde.cnu@gmail.com (Corresponding Author);
msr_eee@vignan.ac.in
[2] Vignan Institute of Technology and Science, Deshmukhi, 508284 Telangana, India,
e-mail: durgasukumar@gmail.com



*How to cite this article:*
Srinivas G., Durga Sukumar G., Subbarao M. Total harmonic distortion analysis of inverter fed induction motor drive using neuro fuzzy type-1 and neuro fuzzy type-2 controllers. *Electrical Engineering & Electromechanics*, 2024, no. 1, pp. 10-16. doi: https://doi.org/10.20998/2074-272X.2024.1.02